Quantum Simulation of Pairing Hamiltonian in Superconductivity

Shirshendu Chatterjee,[1,*] Bikash K. Behera,[2,†] and Felix J. Seo[3,‡]

[1] *Institute of Radio Physics and Electronics, University of Calcutta, Kolkata, India*
[2] *Bikash's Quantum (OPC) Pvt. Ltd., Balindi, Mohanpur 741246, West Bengal, India*
[3] *Department of Physics, Hampton University, Hampton, Virginia, 23668, USA*

Developments in the field of Quantum Computing had achieved remarkable success in recent years. Although a universal quantum computer is still far from reach, the tremendous advances in controllable quantum devices, in particular with solid-state systems, make it possible to physically implement "quantum simulators". Quantum simulators are physical setups able to simulate other quantum systems efficiently that are intractable on classical computers. Based on solid state qubit systems with various types of nearest-neighbor interactions, we propose a complete set of algorithms for simulating pairing Hamiltonian in superconductivity. We realize four different interaction Hamiltonian through IBM superconducting qubit quantum computer for two qubit systems. We studied the fidelity vs iterations in Trotter decomposition. We also analyze the comparison of tunable and constant interactions. Our simulation might be feasible with state-of-the-art technology in solid-state quantum devices.

Keywords: Superconductivity, Pairing Hamiltonians, Quantum simulation, IBM quantum experience

I. INTRODUCTION

Classical computers fail to effectively simulate quantum systems with complex many-body interactions due to the exponential growth of variables for characterizing these systems [1]. Simulating quantum mechanical systems face a great computational problem, especially when dealing with large systems. This difficulty was overcome in 1980's when quantum simulation was proposed to solve such an exponential explosion problem using a controllable quantum system [2]. It was shown in 1996, that a quantum computer only containing few particle interactions can be used to efficiently simulate many body quantum Hamiltonians [4]. Quantum simulation has applications in the study of a variety of problems in a plethora of domains like- starting from condensed-matter physics to high-energy physics [5], quantum chemistry [6] aimed at quantum information processing and quantum gravity [7]. A large number of quantum systems like-neutral atoms [8], ions [9], polar molecules [10], electrons in semiconductors, nuclear spins [9] and photons have been proposed as quantum simulators. Recently, quantum simulators using trapped ions cold atoms [12] and photons have already been experimentally demonstrated to some extent.

Feynman proposed solution to this problem and coined a term with his new concept-quantum computer [3]. In fact, it has made clear over the past three decades, a quantum computer ensured to do much more than simulating quantum mechanics, and therefore in the present world, quantum computation and quantum information theory are very active research fields [16, 17]. Feynman realized at the time that a quantum machine would itself experience an exponential explosion, but with good consequences. The machine would have the capacity to contain an exponentially large amount of information without using an exponentially large amount of physical resources, thus making it a natural tool to perform quantum simulation [13].

In recent years, the interest in quantum simulation has been elevating, and the reason for this is twofold. First, there are a large number of potential applications of quantum simulation in physics [13], chemistry [18] and even biology [19]. Second, the technologies required for the coherent control of quantum systems have matured enough to allow for the physical implementation of practical quantum simulation in the very near future [14]. A great number research groups are now actively focusing at the experimental realization of quantum simulators with tens of qubits, which would be the first practical applications in which quantum computers outperform their classical counterparts [15]. Quantum simulators are classified into analog and digital ones. An analog quantum simulator is a control labile quantum system mimicking the behaviors of the target quantum system whose evolution can be effectively mapped onto the simulator, while a digital quantum simulator normally imitates the time evolution operator of the target system through the implementation of a series of elementary quantum gates. Practically, these two approaches are often used together.

Pairing Hamiltonians, e.g., BCS Hamiltonian [20] in conventional superconductors, feature long-range many-body interactions which are generally intractable on classical computers. Nevertheless, large-scale numerical calculations based on pairing Hamiltonians are of great importance, for instance in mesoscopic condensed matter, ultrasmall metallic grains and heavy nuclei [21]. To tackle this problem, a polynomial time quantum algorithm based on a nuclear magnetic resonance (NMR) [22]

* iamshirshendu98@gmail.com
† bikas.riki@gmail.com
‡ jaetae.seo@hamptonu.edu

quantum computer was proposed, however liquid NMR has several constrains that make NMR quantum computer not scalable. Thus, large-scale implementation of the NMR-based quantum algorithm is unlikely in accordance with the state-of-the-art technology [22].

Superconducting quantum circuits [23] has rapidly progressed in the past decades, thus enabling them to be one of the most promising candidates towards practical quantum information processing. The unique flexibility on design and fabrication of superconducting circuits enables wide tunability in extensive Hamiltonian parameter ranges and the techniques for scaling up are compatible with those for modern integrated circuits. Moreover, the research on other solid-state qubit devices, e.g., quantum dot in semiconductors [24] and defect systems have also made significant progress in the past years.Superconducting qubits have been a leading platform for quantum information processing. These qubits are built from superconducting quantum circuits integrating linear elements, such as capacitors and inductors, together with the only known nonlinear and nondissipative circuit component: the Josephson junction. Superconducting circuits are known to operate at milliKelvin temperatures, where the electromagnetic degrees of freedom associated to currents and voltages in the circuit are described using quantum mechanics.

In the past few decades, awareness has grown in the scientific world that quantum computation may be a more natural and desirable method of computation than the classical one, and the fundamental results may be more easily revealed through the ideas of quantum computation. Feynman's 1982 paper on quantum computing was motivated by the observation that quantum systems seem difficult to simulate on conventional classical computers [16]. The visible difficulty of solving a problem of quantum many-body physics of fermions (and bosons) on a classical computer is the requirement of an exponentially large basis set [25]. Lloyd (1996) showed that a quantum computer [26] can be made of ensembles of qubits $|0\rangle$ and $|1\rangle$ on which quantum gates can act, which can be regarded as a universal quantum simulator [26]. The simulation of an operator requires a platform that is given by IBM Q. With the use of proper analogous quantum gates, most of the operators can be simulated on IBM Q [27, 28]. The IBMQ experience platform provides the general public access to IBM's prototype quantum processors via the cloud. Exploiting the benefits of it, a large number of experiments have been designed to date related to quantum information [37, 38], quantum simulation [39–43], quantum key distribution [44], quantum teleportation [45], quantum cryptography [46, 47], quantum currency [48], quantum devices [49, 50] to name a few. In this paper, we have simulated the many-body pairing models using various Hamiltonians existed in superconductivity. The simulations and the models are suitable for a wide range of models especially superconducting quantum circuits and semiconducting qubit systems. We have computed the quantum state tomography and calculated the fidelity vs. iterations using the Suzuki-Trotter decomposition with graphs for 2 qubits system. We determined the complexity analysis, and studied the time evolution of the system by tuning interaction parameters.

II. MODEL

A. Pairing Hamiltonian in Superconductivity

The BCS pairing Hamiltonian has been widely used in different fields- condensed matter physics, nuclear physics etc. The Hamiltonian is typically expressed in terms of fermionic or bosonic creation (annihilation) operators- $c^\dagger_{\pm m}$ and $c_{\pm l}$ and $n^F_{\pm m} = c^\dagger_{\pm m} c_{\pm m}$ are fermionic number operators.

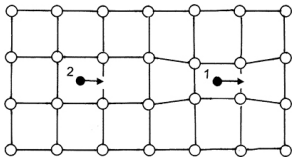

FIG. 1: Pictorial representation of the BCS Pairing Theory . Picture courtesy: Electrons in Solids, Dunlap, Richard A, 2019

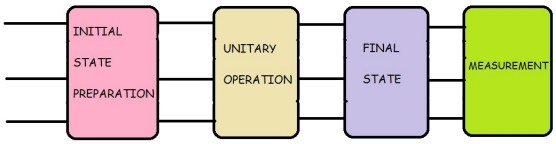

FIG. 2: Schematic diagram of the method of simulation of the 2-qubits pairing Hamiltonian.

The pairing hamitonian is given by-

$$H_{BCS} = \sum_{m=1}^{N} \frac{\epsilon_m}{2}(n^F_m + n^F_{-m}) + \sum_{l=1}^{N}\sum_{m=1}^{N} V_{ml} c^\dagger_m c^\dagger_{-m} c_{-l} c_l \tag{1}$$

where, the matrix elements $V^+_{ml} \equiv \langle m, -m|V|l, -l\rangle$ are real and can be estimated or calculated,e.g.,for superconductors, in terms of Coloumb force and the electron phonon interaction. Pairs of fermions are labeled by the quantum numbers m and $-m$, according to the Cooper pair situation where paired electrons have equal energies but opposite momenta and spins: $m = (\mathbf{p}, \uparrow)$ and $-m = (\mathbf{-p}, \downarrow)$. These are time-reversed and degenerate partners whose energies are considered to be phenomenological parameters.

To convert the concept of BCS hamiltonian to quantum circuits we have to map the fermionic or bosonic operators to qubit operators. As has been analyzed by

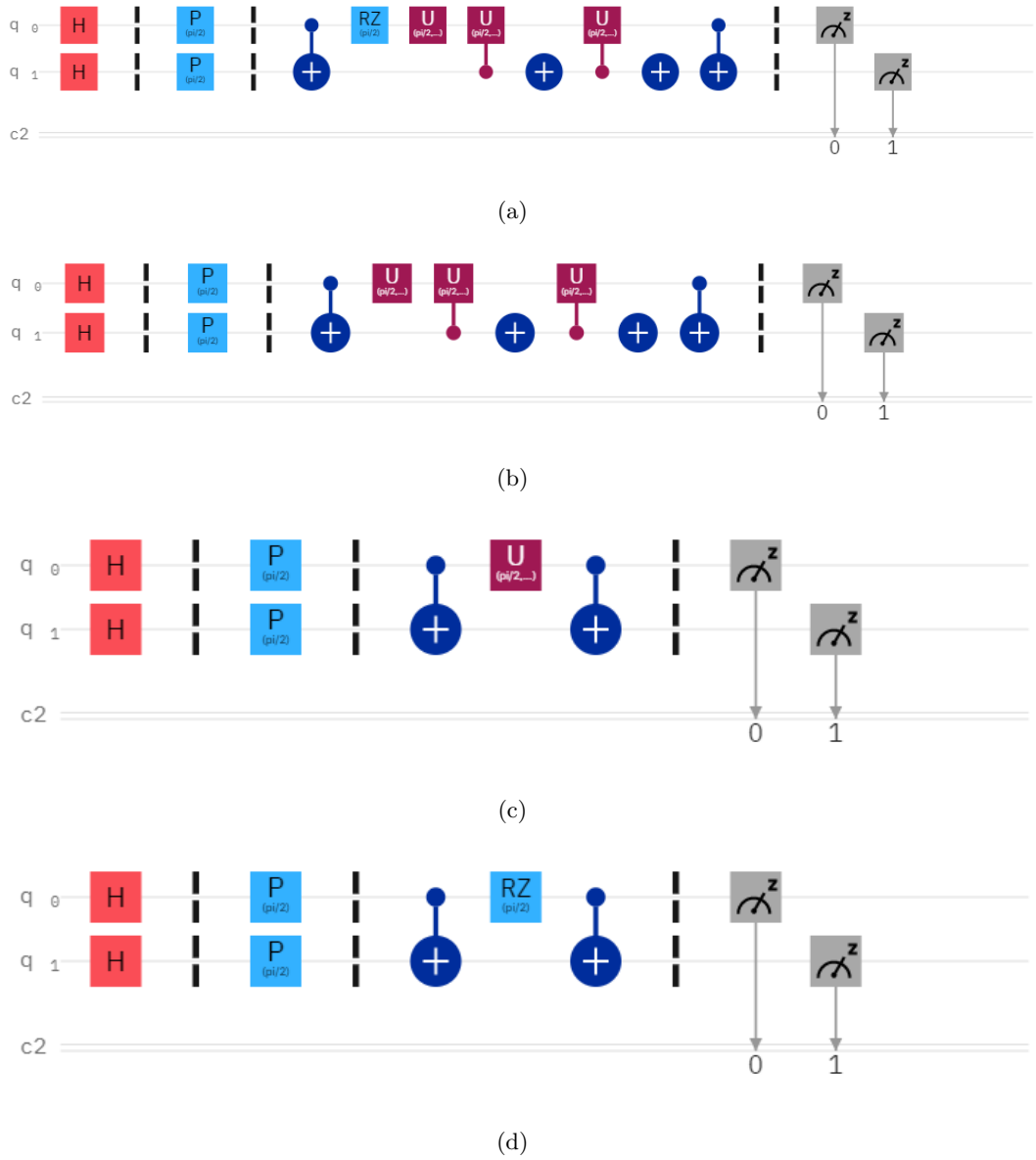

(a)

(b)

(c)

(d)

FIG. 3: (a) Circuit representation of the Heisenberg Nearest-Neighbour Hamiltonian. (b) Circuit representation of the XY Nearest-Neighbour Hamiltonian.(c) Circuit representation of the Transverse Ising Nearest-Neighbour Hamiltonian.(d)Circuit representation of the Longitudinal Ising Nearest-Neighbour Hamiltonian.

the Hamiltonian is mapped into qubit space based on the isomorphic algebras of spin-fermion connection. The fermionic pair operators can be mapped onto qubit operators $\sigma_m^x, \sigma_m^y, \sigma_m^z$ through transformation $\{\sigma_m^x, \sigma_m^y, \sigma_m^z\}$ $= \{c_m^\dagger c_{-m}^\dagger + c_{-m}c_m, ic_{-m}c_m - ic_m^\dagger c_{-m}^\dagger, n_m^F + n_{-m}^F - 1\}$. The Hamiltonian in Eq.(1) can be re-written int the qubit form as-

$$H_p = \sum_{m=1}^{N} \frac{\varepsilon_m}{2}\sigma_m^z + \sum_{m<l} \frac{V_{ml}}{2}(\sigma_m^x\sigma_l^x + \sigma_m^y\sigma_l^y), \tag{2}$$

with $\varepsilon_m = \epsilon_m + V_{mm}$.

B. Nearest Neighbour Coupling Interactions in Superconductivity

Coupling of qubits can be achieved through various type of interactions. For Superconducting Qubits the coupling can be done through many ways such as through inductance, capacitance or Josephson junctions. The interaction models can be classified into four categories- XY Model, Heisenberg Model, Transverse Ising Model

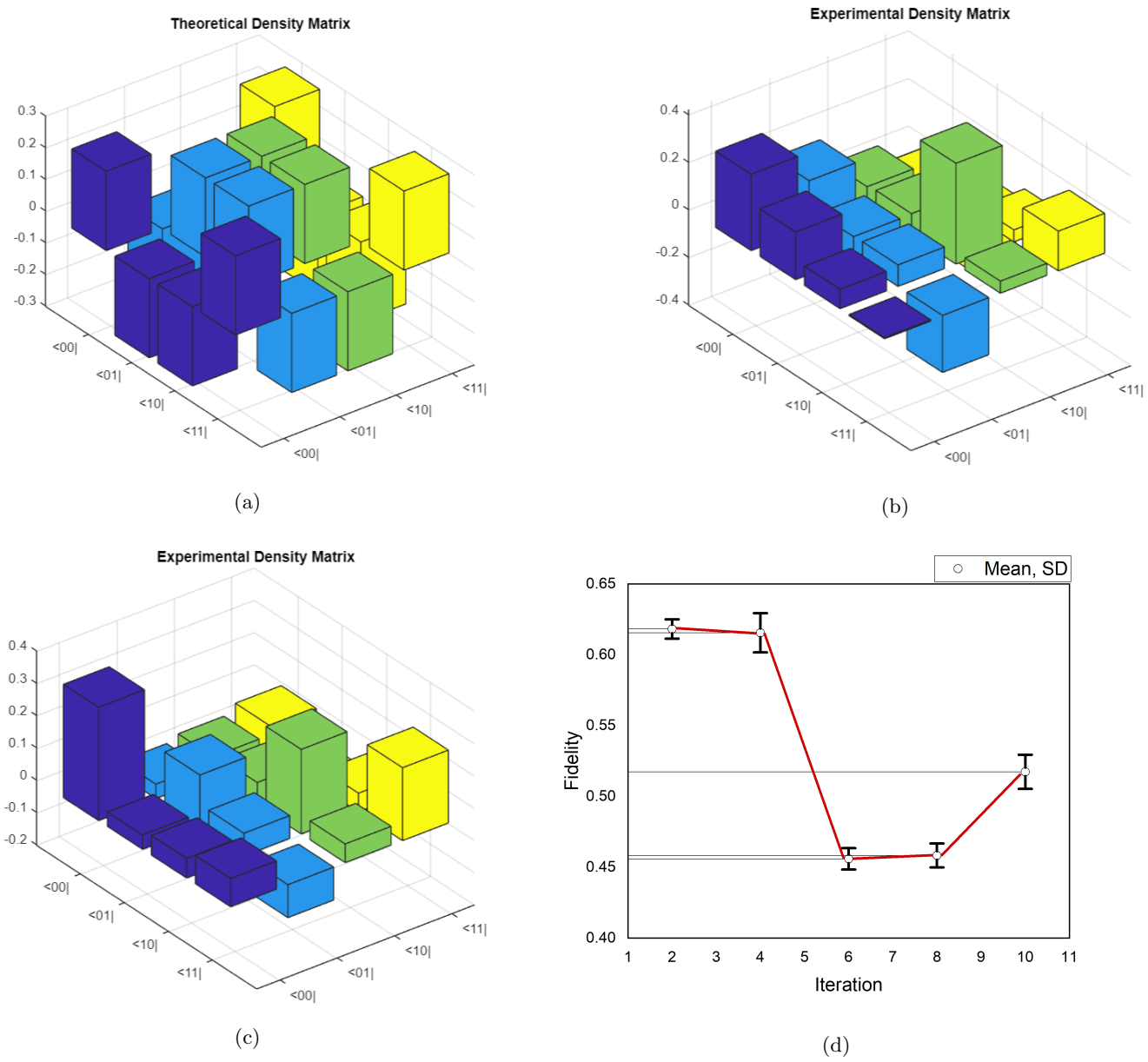

(a) (b) (c) (d)

FIG. 4: (a) Theoretical Density Matrix for Heisenberg Model. (b) Experimental Density Matrix for 2 Iteration.(c) Experimental Density Matrix for 10 Iteration.(d) Fidelity vs Iteration for iteration ranging from 2 to 10.

TABLE I: Interaction Hamiltonians for the four different models

Interaction Models	**Interactions Hamiltonians**
XY model	$H_{XY} = H_0 + \sum_{i=x,y} \sum_{l=1}^{N-1} J_l \sigma_l^i \sigma_{l+1}^i$
Heisenberg model	$H_H = H_0 + \sum_{i=x,y,z} \sum_{l=1}^{N-1} J_l^i \sigma_l^i \sigma_{l+1}^i$
Transverse Ising model	$H_{Ising,T} = H_0 + \sum_{l=1}^{N-1} J_l \sigma_l^x \sigma_{l+1}^x$
Longitudinal Ising model	$H_{Ising,L} = H_0 + \sum_{l=1}^{N-1} J_l \sigma_l^z \sigma_{l+1}^z$

and Longitudinal Ising Model. These four type of Hamiltonian can be written together as-

$$H = H_0 + H_I \tag{3}$$

with H_0 denoting the single-qubit Hamiltonian.

$$H_0 = \sum_{l=1}^{N} \frac{1}{2} \omega_l \sigma_l^z \tag{4}$$

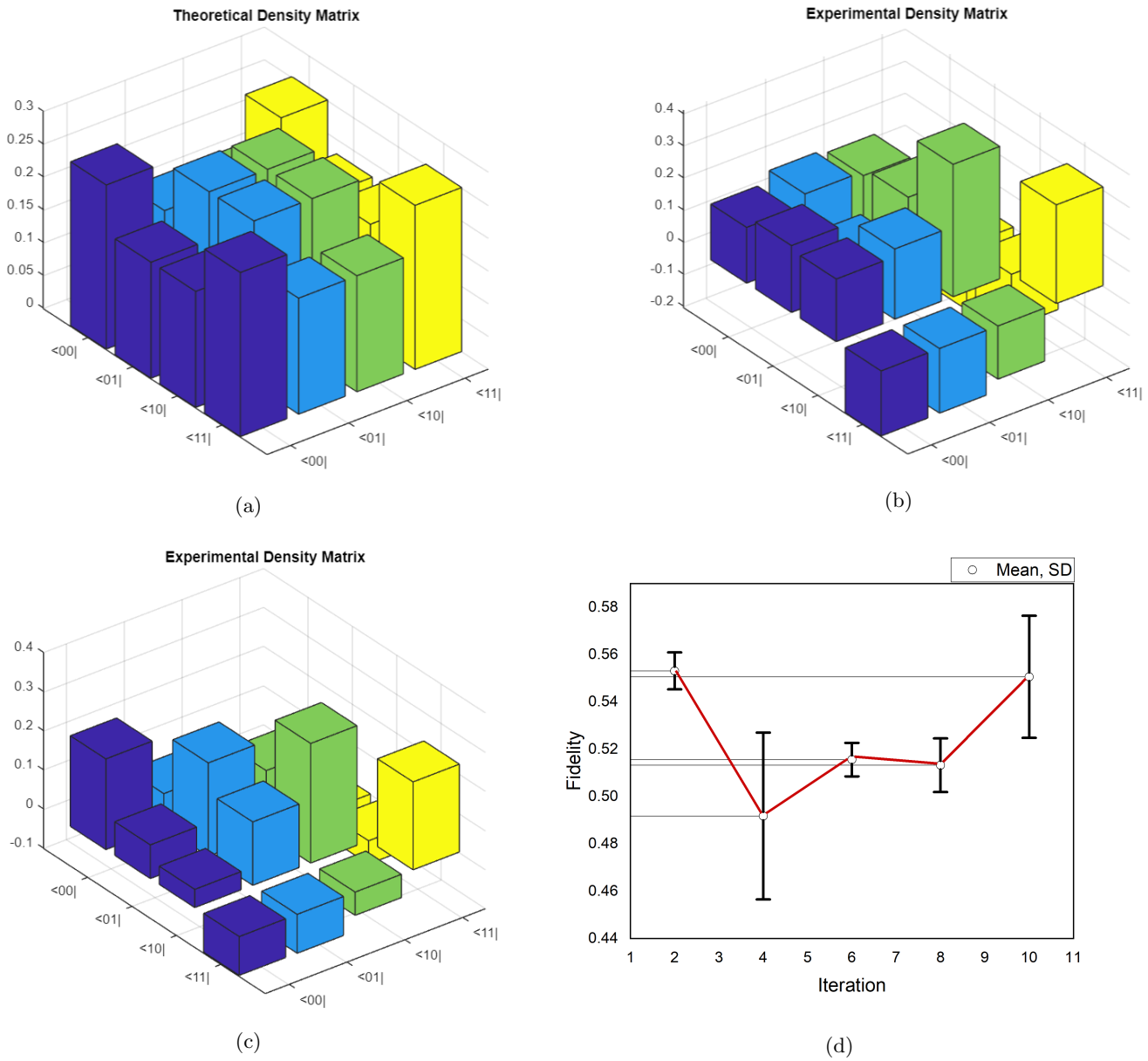

(a) (b) (c) (d)

FIG. 5: (a) Theoretical Density Matrix for XY Model. (b) Experimental Density Matrix for 2 Iteration.(c) Experimental Density Matrix for 10 Iteration.(d) Fidelity vs Iteration for iteration ranging from 2 to 10.

and H_I denoting the interation Hamiltonian

$$H_I = \sum_{l=1}^{N-1} (J_l^x \sigma_l^x \sigma_{l+1}^x + J_l^y \sigma_l^y \sigma_{l+1}^y + J_l^z \sigma_l^z \sigma_{l+1}^z) \tag{5}$$

Here $\sigma_l^x, \sigma_l^y, \sigma_l^z$ are Pauli matrices in the basic of σ_l^z and l denotes the lth qubit. The coupling strength between the lth and the $(l+1)$th qubits is denoted by $J_l (l = 1, ..., N-1)$.

The parameters of the previous two equations are chosen to get the Hamiltonian of four different models and J_l is fixed accordingly. It can be seen that the pairing models in Eq.(2) does not follow the form of the Hamiltonians of Eq.(3). Thus it is imperative to design algorithms to simulate these pairing Hamiltonians using the four types of interaction Hamiltonian.

For the operators $\sigma_m^x, \sigma_m^y, \sigma_m^z$ it should be taken care when simulating in the Suzuki-Trotter decoposition as the operators may not commute.We note that the tunability of parameters $\omega_l (l = 1, ..., N)$ and $J_l^x (i = x, y, z; l = 1, ..., N-1)$ affects the efficiency of the algorithms.

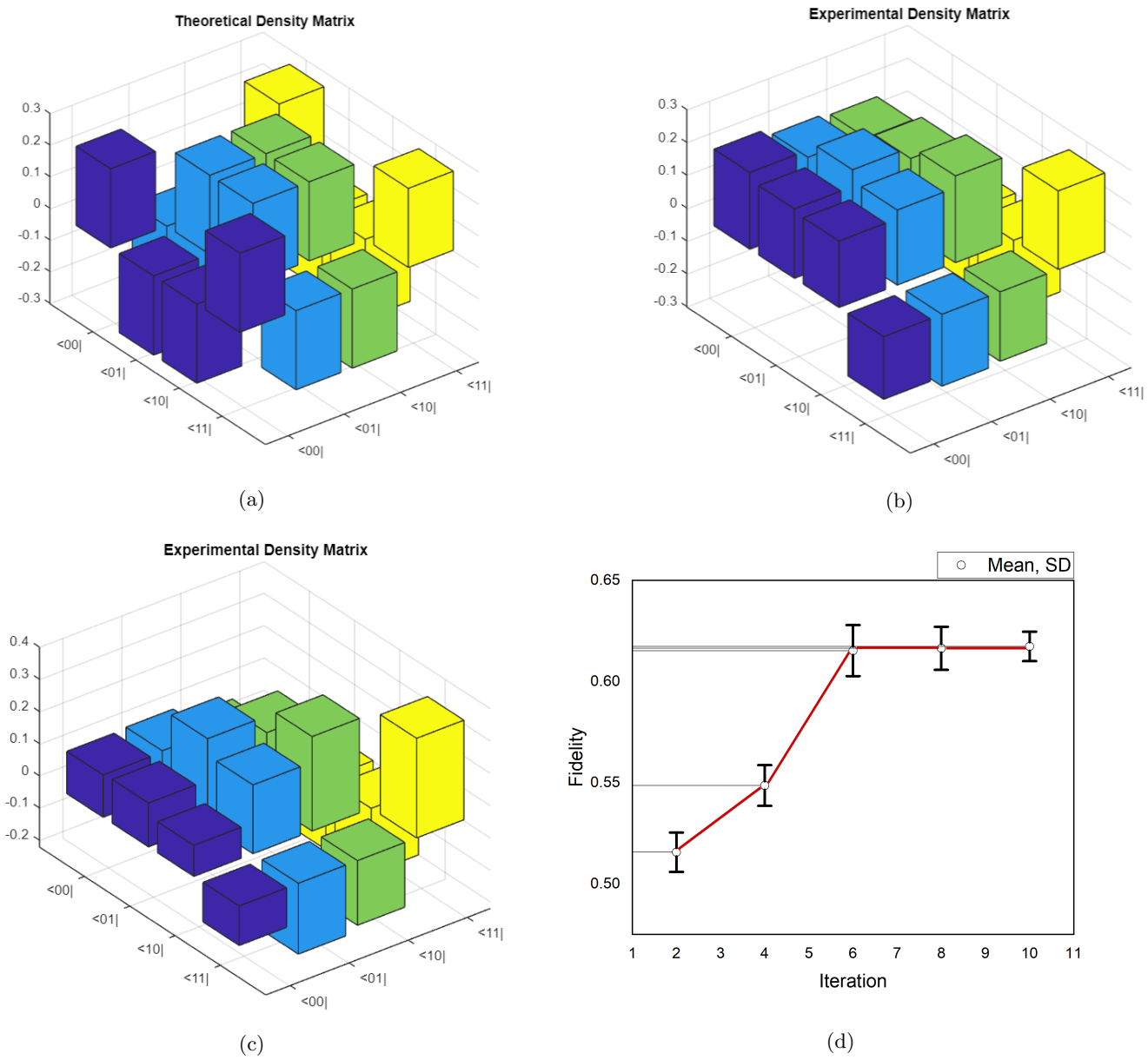

(a) (b) (c) (d)

FIG. 6: (a) Theoretical Density Matrix for Transverse Ising Model. (b) Experimental Density Matrix for 2 Iteration.(c) Experimental Density Matrix for 10 Iteration.(d) Fidelity vs Iteration for iteration ranging from 2 to 10.

III. SIMULATION OF HAMILTONIAN OPERATOR

Given the initial state at time t=0, we can solve it to obtain the state at any later instant [55]. If $\hat{H}$ is independent of time, then

$$|\psi(x,t)\rangle = e^{-i\hat{H}t/\hbar}\,|\psi(0)\rangle \tag{6}$$

Where $U(t) = e^{-i\hat{H}t/\hbar}$, is the time evolution operator. U(t) is a unitary operator, i.e., $U^{\dagger}U = \mathbb{I}$. For our case we have to simulate four different Hamiltonian thus finding the corresponding unitary operations to build the quantum circuit. In general if we try to find the matrices for the time evolution operator we will have to find how the terms $\hat{\sigma}^x, \hat{\sigma}^y, \hat{\sigma}^z, \hat{\sigma}^x\hat{\sigma}^x, \hat{\sigma}^y\hat{\sigma}^y$ and $\hat{\sigma}^z\hat{\sigma}^z$ look like. We can write separate terms for x, y and z as $\hat{\sigma}^x\hat{\sigma}^x$, $\hat{\sigma}^y\hat{\sigma}^y$ and $\hat{\sigma}^z\hat{\sigma}^z$ commute with each other. The Hamiltonian of our choice is-

$$H = \sum_{l=1}^{N} \frac{1}{2}\omega_l \sigma_l^z + \sum_{l=1}^{N-1} (J_l^x \sigma_l^x \sigma_{l+1}^x + J_l^y \sigma_l^y \sigma_{l+1}^y + J_l^z \sigma_l^z \sigma_{l+1}^z) \tag{7}$$

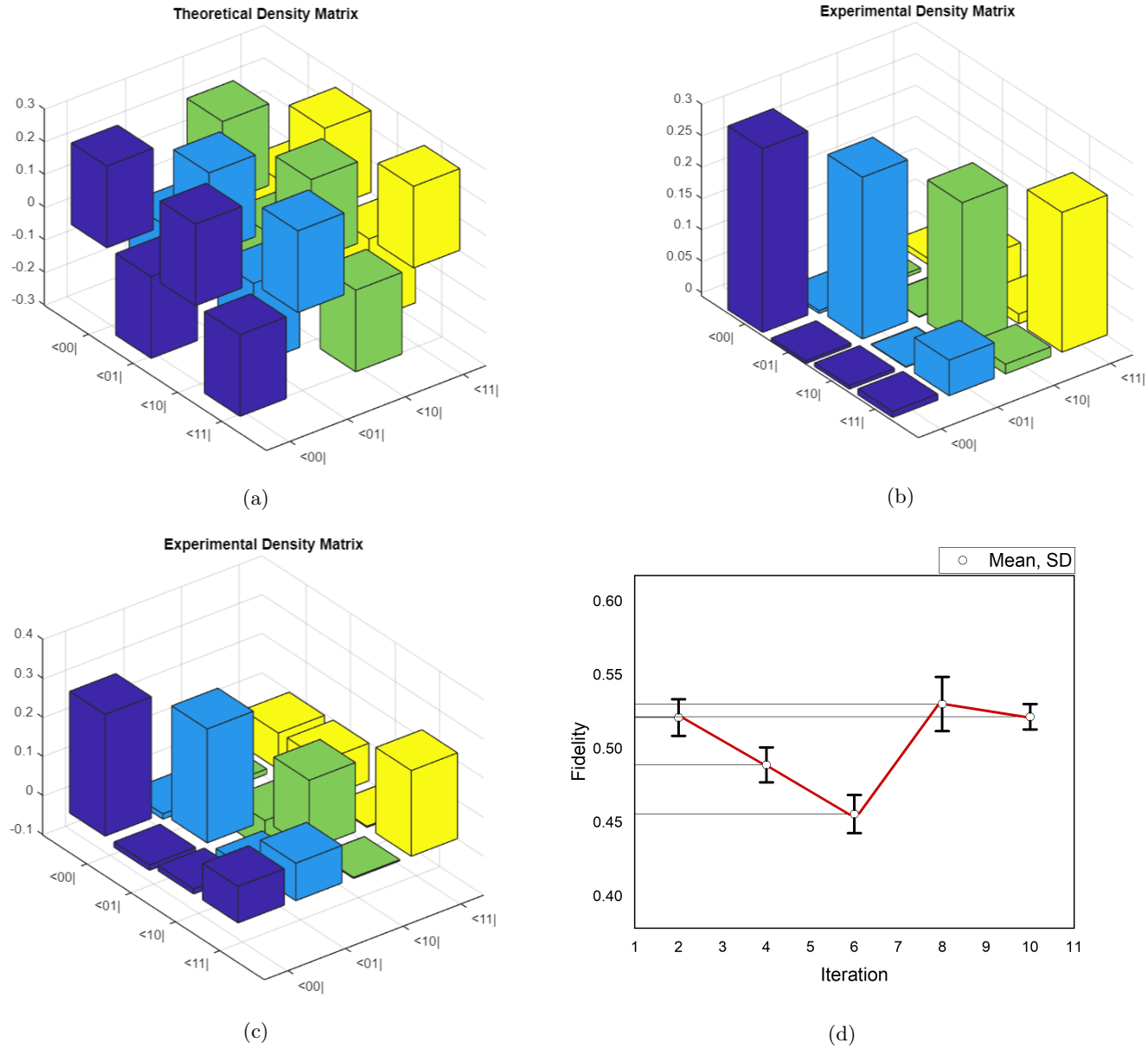

(a) (b) (c) (d)

FIG. 7: (a) Theoretical Density Matrix for Longitudinal Ising Model. (b) Experimental Density Matrix for 2 Iteration.(c) Experimental Density Matrix for 10 Iteration.(d) Fidelity vs Iteration for iteration ranging from 2 to 10.

The corresponding time evolution operator is given by-

$$U(t) = e^{-i(\sum_{l=1}^{N} \frac{1}{2}\omega_l \sigma_l^z)t} e^{-i\sum_{l=1}^{N-1}(J_l^x \sigma_l^x \sigma_{l+1}^x + J_l^y \sigma_l^y \sigma_{l+1}^y + J_l^z \sigma_l^z \sigma_{l+1}^z)t} \tag{8}$$

Here, $\hat{\sigma}^x = \begin{bmatrix} 0 & 1 \\ 1 & 0 \end{bmatrix}$, $\hat{\sigma}^y = \begin{bmatrix} 0 & -i \\ i & 0 \end{bmatrix}$, and $\hat{\sigma}^z = \begin{bmatrix} 1 & 0 \\ 0 & -1 \end{bmatrix}$

We can write the first part of the operator as per the value of pauli matrix($\hat{\sigma}^z$) shown.

The term $e^{-iJ_l\hat{\sigma}^x\hat{\sigma}^x t}$ in the second part of the operator, can be written as,

$\mathbb{I}cos\ J_1 t - \hat{\sigma}^x \bigotimes \hat{\sigma}^x isin\ J_1 t$

$$= \begin{bmatrix} cos(J_l t) & 0 & 0 & -isin(J_l t) \\ 0 & cos(J_l t) & -isin(J_l t) & 0 \\ 0 & -isin(J_l t) & cos(J_l t) & 0 \\ -isin(J_l t) & 0 & 0 & cos(J_l t) \end{bmatrix} \tag{9}$$

The term $e^{-iJ_l\hat{\sigma}^y\hat{\sigma}^y t}$in the second part of the operator can be written as,

$\mathbb{I}cos\ J_l t - \hat{\sigma}^y \bigotimes \hat{\sigma}^y isin\ J_l t$

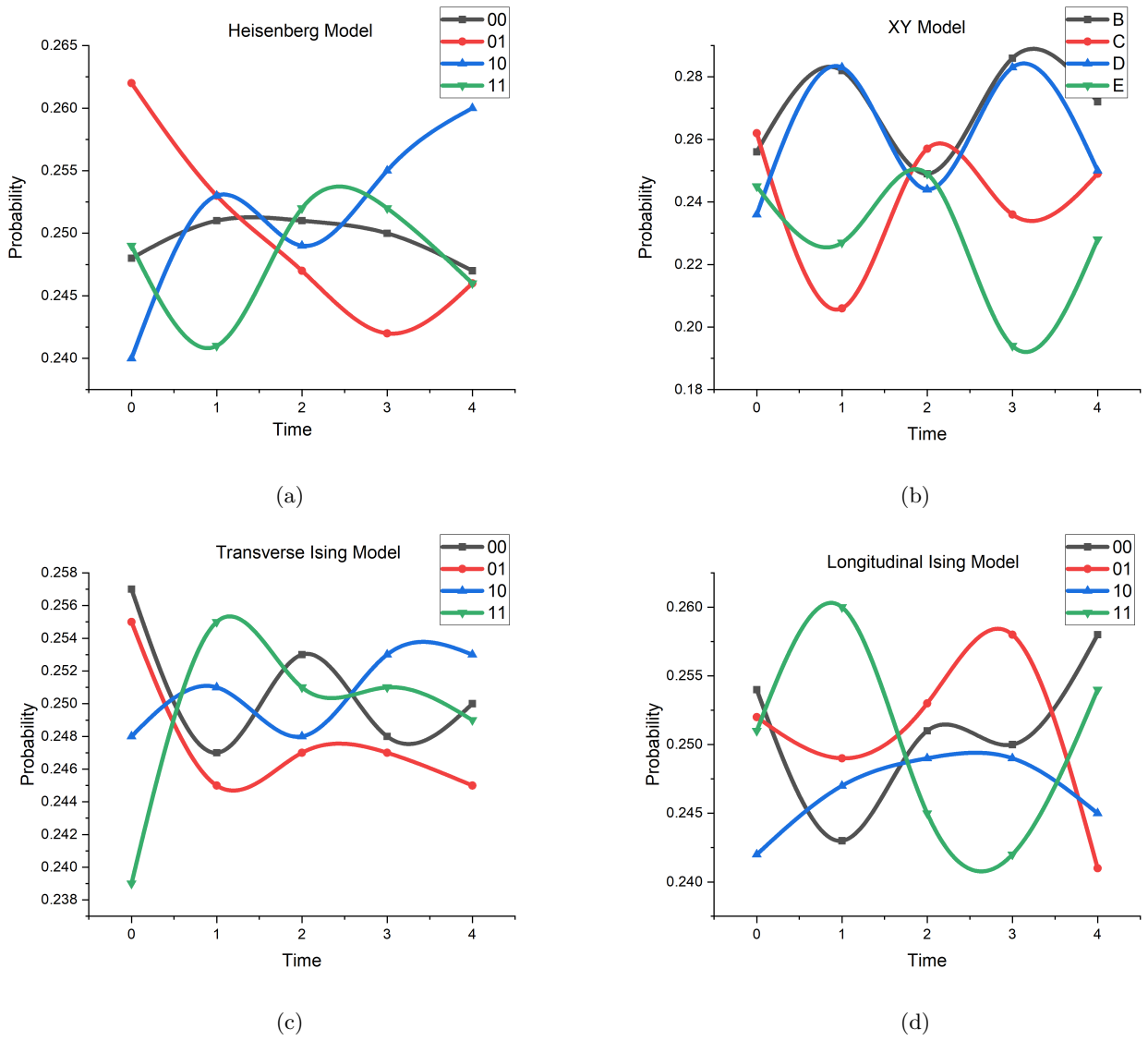

FIG. 8: Time Evolution of different Models at $\theta = \frac{\pi}{2}$ -(a)Heisenberg Model. (b) XY Model. (c) Transverse Ising Model. (d) Longitudinal Ising Model.

$$= \begin{bmatrix} cos(J_l t) & 0 & 0 & isin(J_l t) \\ 0 & cos(J_l t) & -isin(J_l t) & 0 \\ 0 & -isin(J_l t) & cos(J_l t) & 0 \\ isin(J_l t) & 0 & 0 & cos(J_l t) \end{bmatrix} \quad (10)$$

The term $e^{-iJ_l \hat{\sigma}^z \hat{\sigma}^z t}$ in the second part of the operator can be written as,

$\mathbb{I} cos\ J_l t - \hat{\sigma}^z \bigotimes \hat{\sigma}^z isin\ J_l t$

$$= \begin{bmatrix} e^{-iJ_l t} & 0 & 0 & 0 \\ 0 & e^{iJ_l t} & 0 & 0 \\ 0 & 0 & e^{iJ_l t} & 0 \\ 0 & 0 & 0 & e^{-iJ_l t} \end{bmatrix} \quad (11)$$

Now, referring to the four Hamiltonian's, we can write the time evaluation operator and thus proceed to implement. Each of these four types of Hamiltonians is a special case of Eq.(8) with parameters being properly chosen.The Hamiltonian can be thus reduced to (i) Longitudinal Ising Hamiltonian for parameters $J_l^x = J_l^y = 0$ and $J_l^z = J_l$; (ii)Transverse Ising Hamiltonian for parameters $J_l^y = J_l^z = 0$ and $J_l^x = J_l$;(iii)XY Hamiltonian for parameters $J_l^z = 0$ and $J_l^x = J_l^y = J_l$; (iv)Heisenberg Hamiltonian for parameters$J_l^x = J_l^y = J_l^z = J_l$. For 2 qubit system, the parameter l will range 1 to 2 to account for the coupling between qubits. The following step is to implement the unitary operator as obtained from the previous calculations in an order to the initial superposed state and obtain the time evolution of the Hamiltonian.

So if we elaborate the whole calculation-

In General

The Hamiltonian is-

$$H = \sum_{l=1}^{N} \frac{1}{2}\omega_l \sigma_l^z + \sum_{l=1}^{N-1} (J_l^x \sigma_l^x \sigma_{l+1}^x + J_l^y \sigma_l^y \sigma_{l+1}^y + J_l^z \sigma_l^z \sigma_{l+1}^z) \tag{12}$$

We have to decompose them. So for 2 Qubit system the Hamiltonian looks like-

$$H = \frac{1}{2}\omega_1 \sigma_1^z + \frac{1}{2}\omega_1 \sigma_2^z + (J_1^x \sigma_1^x \sigma_2^x + J_1^y \sigma_1^y \sigma_2^y + J_1^z \sigma_1^z \sigma_2^z) \tag{13}$$

Now we can see there are interraction between 1st and second qubit. So the calculation is as follows-

For $\sigma_1^x \sigma_2^x$ term,

$\mathbb{I} cos\ J_1 t - \hat{\sigma}^x \bigotimes \hat{\sigma}^x isin\ J_1 t$

$$= \begin{bmatrix} cos(J_1 t) & 0 & 0 & -isin(J_1 t) \\ 0 & cos(J_1 t) & -isin(J_1 t) & 0 \\ 0 & -isin(J_1 t) & cos(J_1 t) & 0 \\ -isin(J_1 t) & 0 & 0 & cos(J_1 t) \end{bmatrix} \tag{14}$$

This cannot be decomposed into single qubit gates.So, we will try to apply it on 2 qubit states so to decompose them into basic gates for implementation. Let us apply on two qubit basis states. Thus we get-
$|00\rangle \rightarrow cost\,|00\rangle - isint\,|11\rangle$
$|01\rangle \rightarrow cost\,|01\rangle - isint\,|10\rangle$
$|10\rangle \rightarrow -isint\,|01\rangle + cost\,|10\rangle$
$|11\rangle \rightarrow -isint\,|00\rangle + cost\,|11\rangle$

both are in entanglement and superposition. So, first lets remove the entanglement by applying a CNOT gate,
$(\text{cost}|0\rangle - isint\,|1\rangle)\,|0\rangle$
$(cost\,|0\rangle - isint\,|1\rangle)\,|1\rangle$
$(-isint\,|0\rangle + cost\,|1\rangle)\,|1\rangle$
$(-isint\,|0\rangle + cost\,|1\rangle)\,|0\rangle$

Now, lets remove superposition. We need to find a operation which when applied on $|0\rangle$ will give cost$|0\rangle$-isint$|1\rangle$ and when applied to $|1\rangle$ will give -isint$|0\rangle$+cost$|1\rangle$.

Let us consider the U3 gate

$$U3(\theta, \phi, \lambda) = \begin{bmatrix} cos\theta/2 & -e^{i\lambda} sin\theta/2 \\ e^{i\phi} sin\theta/2 & e^{i(\phi+\lambda)} cos\theta/2 \end{bmatrix} \tag{15}$$

Now if we put $\phi = \frac{-\pi}{2}$ and $\lambda = \frac{\pi}{2}$, then U3 gate becomes,

$$U3(\theta, \phi, \lambda) = \begin{bmatrix} cos\frac{\theta}{2} & -isin\frac{\theta}{2} \\ -isin\frac{\theta}{2} & cos\frac{\theta}{2} \end{bmatrix} \tag{16}$$

This one satisfies the above conditions. Then the state before the application of U3 Gate should be - $|00\rangle$, $|01\rangle$, $|11\rangle$, $|10\rangle$. But to make then in the correct order, we again apply a CNOT gate.

Thus, $e^{-iJ_l \hat{\sigma}^x \hat{\sigma}^x t} = (CNOT)_{12}.U3_1\ (CNOT)_{12}$

Similarly, for $\sigma_1^y \sigma_2^y$ term,

$\mathbb{I} cos\ J_1 t - \hat{\sigma}^y \bigotimes \hat{\sigma}^y isin\ J_1 t$

$$= \begin{bmatrix} cos(J_1 t) & 0 & 0 & isin(J_1 t) \\ 0 & cos(J_1 t) & -isin(J_1 t) & 0 \\ 0 & -isin(J_1 t) & cos(J_1 t) & 0 \\ isin(J_1 t) & 0 & 0 & cos(J_1 t) \end{bmatrix} \tag{17}$$

This cannot be decomposed into single qubit gates. So, we will try to apply it on 2 qubit states so to decompose them into basic gates for implementation. Let us apply on two qubit basis states. Thus we get-
$|00\rangle \rightarrow cost\,|00\rangle + isint\,|11\rangle$
$|01\rangle \rightarrow cost\,|01\rangle - isint\,|10\rangle$
$|10\rangle \rightarrow -isint\,|01\rangle + cost\,|10\rangle$
$|11\rangle \rightarrow isint\,|00\rangle + cost\,|11\rangle$

both are in entanglement and superposition. So, first lets remove the entanglement by applying a CNOT gate,
$(\text{cost}|0\rangle + isint\,|1\rangle)\,|0\rangle$ .....(i)
$(cost\,|0\rangle - isint\,|1\rangle)\,|1\rangle$ .....(ii)
$(-isint\,|0\rangle + cost\,|1\rangle)\,|1\rangle$ .....(iii)
$(isint\,|0\rangle + cost\,|1\rangle)\,|0\rangle$ .....(iv)

Now, lets remove superposition. We need to find a U3 gate. Among four types of U3 gates only the two shown below can be applied.

$$U3 = \begin{bmatrix} cos\frac{\theta}{2} & isin\frac{\theta}{2} \\ isin\frac{\theta}{2} & cos\frac{\theta}{2} \end{bmatrix} \tag{18}$$

$$U3^\dagger = \begin{bmatrix} cos\frac{\theta}{2} & -isin\frac{\theta}{2} \\ -isin\frac{\theta}{2} & cos\frac{\theta}{2} \end{bmatrix} \tag{19}$$

It can be observed that on **(i)** and **(iv)** position U3 has to be applied and on **(ii)** and **(iii)** position $U3^\dagger$ has to be applied. We can notice that on **(i)** and **(iv)** the second qubit is in $|0\rangle$ state and on **(ii)** and **(iii)**the second qubit is on $|1\rangle$ state. So, we can use the second qubit as the control qubit and apply the above U3 gates.

Now the state just before the control and the anti-control U3 gates would be- $|00\rangle$, $|01\rangle$, $|11\rangle$, $|10\rangle$. But to make then in the correct order, we again apply a CNOT gate.

Thus, $e^{-iJ_l \hat{\sigma}^y \hat{\sigma}^y t} = (CNOT)_{12}.U3_{21}.\ U3_{21}^\dagger\ (CNOT)_{12}$.

Similarly for $\sigma_1^z \sigma_2^z$ term,

$\mathbb{I} cos\ J_1 t - \hat{\sigma}^z \bigotimes \hat{\sigma}^z isin\ J_1 t$

$$= \begin{bmatrix} e^{-iJ_1 t} & 0 & 0 & 0 \\ 0 & e^{iJ_1 t} & 0 & 0 \\ 0 & 0 & e^{iJ_1 t} & 0 \\ 0 & 0 & 0 & e^{-iJ_1 t} \end{bmatrix} \tag{20}$$

Let us apply on two qubit basis states. Thus we get-
$|00\rangle \rightarrow e^{-it}|00\rangle$
$|01\rangle \rightarrow e^{it}|01\rangle$
$|10\rangle \rightarrow e^{it}|10\rangle$
$|11\rangle \rightarrow e^{-it}|11\rangle$

So, first lets remove the entanglement by applying a CNOT gate. Thus we get-
$(e^{-it}|0\rangle)\,|0\rangle$
$(e^{it}|0\rangle)\,|1\rangle$
$(e^{it}|1\rangle)\,|1\rangle$
$(e^{-it}|1\rangle)\,|0\rangle$

We need to find a operation which when applied on $|0\rangle$ will give $e^{-it}\,|0\rangle$ and when applied to $|1\rangle$ will give $e^{it}\,|1\rangle$. RZ= [exp(-1i*theta/2) 0; 0 exp(1i*theta/2)];
Let us consider the Rz gate

$$Rz(\theta) = \begin{bmatrix} e^{-i\frac{\theta}{2}} & 0 \\ 0 & e^{i\frac{\theta}{2}} \end{bmatrix} \tag{21}$$

This one satisfies the above conditions. Then the state before the application of U3 Gate should be - $|00\rangle$, $|01\rangle$, $|11\rangle$, $|10\rangle$. But to make then in the correct order, we again apply a CNOT gate.

Doing the calculations , we observe, that

$e^{-iJ_l\hat{\sigma}^z\hat{\sigma}^z t} = (CNOT)_{12}.Rz_1.\ (CNOT)_{12}$.
Thus, we complete the circuit for the Hamiltonian in general. Now, we can extend the calculation for the Heisenberg Model, XY Model, Transverse Ising Model, Longitudinal Ising Model. The
The Hamiltonians of all the models for 2 qubit system is shown below.

Heisenberg Model

$$H = \frac{1}{2}\omega_1\sigma_1^z + \frac{1}{2}\omega_1\sigma_2^z + (J_1^x\sigma_1^x\sigma_2^x + J_1^y\sigma_1^y\sigma_2^y + J_1^z\sigma_1^z\sigma_2^z) \tag{22}$$

XY Model

$$H = \frac{1}{2}\omega_1\sigma_1^z + \frac{1}{2}\omega_1\sigma_2^z + (J_1^x\sigma_1^x\sigma_2^x + J_1^y\sigma_1^y\sigma_2^y) \tag{23}$$

Transverse Ising Model

$$H = \frac{1}{2}\omega_1\sigma_1^z + \frac{1}{2}\omega_1\sigma_2^z + J_1^x\sigma_1^x\sigma_2^x \tag{24}$$

Longitudinal Ising Model

$$H = \frac{1}{2}\omega_1\sigma_1^z + \frac{1}{2}\omega_1\sigma_2^z + J_1^z\sigma_1^z\sigma_2^z \tag{25}$$

IV. IMPLEMENTATION ON IBM QUANTUM EXPERIENCE

A. Initial state preparation and unitary operation

The initial state is prepared by superposing the states of all the three qubits required to define the Hamiltonian as per the superconducting pairing models.
This is done by putting a Hadamard gate on each qubit. This will provide contribution of all the qubits to the measurement.The unitary operators obtained in the previous section corresponding to the XX, YY, and ZZ type of interaction are then converted into quantum gates [17] and applied to form a circuit.

- For XX type of interaction:
  Comparing with the standard U_3 gate i.e,

$$U3(\theta,\phi,\lambda) = \begin{bmatrix} cos\theta/2 & -e^{i\lambda}sin\theta/2 \\ e^{i\phi}sin\theta/2 & e^{i(\phi+\lambda)}cos\theta/2 \end{bmatrix} \tag{26}$$

  We find the parameters for the gate to be used as:
  $\theta = 2J_lt$, $\phi = -\pi/2$ and $\lambda = \pi/2$.

- For YY type of interaction:
  Parameters obtained for $U3$ gate:
  $\theta = 2J_lt$, $\phi = -\pi/2$ and $\lambda = \pi/2$.
  Parameters obtained for $U3^\dagger$ gate:
  $\theta = 2J_lt$, $\phi = \pi/2$ and $\lambda = -\pi/2$.

- For ZZ type of interaction: Comparing with the standard $U1$ gate, i.e.,

$$U1(\lambda) = \begin{bmatrix} 1 & 0 \\ 0 & e^{i\lambda} \end{bmatrix} \tag{27}$$

  we get the parameter $\lambda = 2J_lt$.

B. Using Quantum State Tomography for Suzuki-Trotter Decomposition of Quantum Circuit

In this section, we take a look at use of Suzuki-Trotter decomposition to count the fidelity vs. the number of iterations of the quantum circuit. The circuit was iterated for $n = 2, 4, 6, 8, 10$. We have used Quantum State Tomography [59] to get the theoretical and experimental density matrices, thus calculating the fidelity of the circuit.
The general form of Quantum State Tomography is given by-

$$\rho = \frac{1}{2^N}\sum_{l=i_1,i_2,...,i_N=0}^{3} T_{i_1,i_2,...,i_N}\sigma_{i_1}\otimes\sigma_{i_2}\otimes...\sigma_{i_N} \tag{28}$$

The experimental matrices of the circuits were computed through the density matrix as shown above. The

experimental density matrix and the theoretical density matrix were compared and the fidelity of the quantum circuits were thus calculated. The whole circuit has been simulated in ' IBMQ-Lima'.

V. MEASUREMENTS AND RESULTS

Probabilistic simulations and related calculations of quantum systems are usually carried out using the Monte Carlo method on a classical computer [25]. Such methods were devised to overcome the setback offered by exponentially growing phase spaces. Whereas, a quantum simulator [58] is usually very much under control of the experimenter. It is capable of simulating the dynamical behaviours of the physical model under inspection. Irrespective of the degree of internal correlations or entanglement between the degrees of freedom of the model, it can perform its job efficiently [57]. In this Section, the results corresponding to the different circuits designed during our attempt of quantum simulation of the Pairing Hamiltonian in Superconductivity are provided.

Fig.4 shows the theoretical density matrix and the experimental density matrix of Heisenberg Model .The fidelity vs. iteration of the circuit is also plotted. The matrices and the graphs are also plotted for XY Model, Transverse Ising Model, Longitudinal Model in Fig.5,Fig.6,Fig.7 respectively.

It can be seen in Fig.4,that for the Heisenberg Model the experimental density matrix deviates clearly from the theoretical density matrix. There can be changes which can be seen in the experimental density matrix also as the number of iteration is increased. The fidelity thus found is seen to decrease from 2 iteration to 6, again increasing till 10 iteration. The error for every iteration is checked and a graph has been plotted to check the trend of variation.

In Fig.5, for XY model it was seen that the experimental density matrix changed as the iteration increased. As per the fidelity vs. iteration plot, the fidelity which decreases from 2 iteration till 4 iteration, increases to 6 iteration and attain the higher value at 10 iteration. The graph shows the trend of the change.

For Transverse Ising Model(Fig.6) it was seen the experimental density matrix figures also changed for increasing iteration. The fidelity of the circuit increased rapidly from 2 iteration to 4 iteration but after that remained to be near constant from 6-10 iteration.

Lastly for Longitudinal Ising Model(Fig.7) the experimental density matrix changed for increasing iteration from 2-10. The fidelity of the circuit decreased from 2-6 iteration, slightly increased till 8 iteration and again decreased till 10 iteration.

The variation of the fidelity shown for the four models can be accounted to the inclusion of noise from the real chip Quantum Computer. In theory, if the number of gates increase in a circuit, due to inclusion of more noise, it is expected the fidelity to decrease. But, in experimental regime, this trend may be affected and can also give fidelity higher for systems with more number of gates, as seen in some models above.

Fig.8 shows the variation of probability of possible states with respect to different values at $\theta = \frac{\pi}{2}$ and the time varies for t=0,..,4.

VI. CONCLUSION

In summary, we have studied algorithms and circuits for simulating the pairing Hamiltonians based on various nearest-neighbor interactions, e.g., Heisenberg Hamiltonian, longitudinal Ising Hamiltonian, XY Hamiltonian and transverse Ising Hamiltonian, which are available in the solid-state quantum devices. The Hamiltonians are all been implemented on IBM superconducting qubit quantum computer. We have analyzed the probability change for time evolution and also found out the Quantum State Tomography for the different Hamiltonian thus finding the fidelity vs. iterations of the different circuits using Suzuki-Trotter decomposition. The fidelity shows varied pattern for different interaction models in superconductivity.

ACKNOWLEDGEMENT

The authors acknowledge the support of IBM Quantum Experience for providing the access of quantum processors. The views expressed are those of the authors and do not reflect the official policy or position of IBM or IBM Quantum Experience team.

[1] A.Smith, M.S.Kim, F.Pollmann, et al. Simulating quantum many-body dynamics on a current digital quantum computer. npj Quantum Inf 5, **106** (2019).

[2] S. G. Schirmer, I. C. H. Pullen, A. I. Solomon Controllability of Quantum Systems IFAC Proceedings Volume **36**, Issue 2, (2003)

[3] R.P. Feynman, Simulating physics with computers. Int J Theor Phys **21**, 467–488 (1982).

[4] A. Shabani, M. Mohseni, S. Lloyd, R. L. Kosut, and H. Rabitz Estimation of many-body quantum Hamiltonians via compressive sensing Phys. Rev. A **84**, 012107 (2011)

[5] C W. Bauer, Wibe A. de Jong, B. Nachman, D. Provasoli A quantum algorithm for high energy physics simulations Phys. Rev. Lett. **126**, 062001 (2021)

[6] Dawei Lu, Boruo Xu, Nanyang Xu, Zhaokai Li, Hongwei Chen, Xinhua Peng, Ruixue Xua and Jiangfeng Du, Quantum chemistry simulation on quantum computers: theories and experiments Phys. Chem. Chem. Phys.,**14**, 9411-9420 (2012)

[7] L. Cohen, A. J. Brady, Z. Huang, H. Liu, D. Qu, J. P. Dowling, and M. Han Phys. Rev. Lett. **126**, 020501 (2021)

[8] M. Saffman, Quantum computing with neutral atoms, National Science Review, Volume **6**, Issue 1, Pages 24–25 (2019)

[9] V.Salari, H. Naeij A. Shafiee, Quantum Interference and Selectivity through Biological Ion Channels. Sci Rep **7**, 41625 (2017).

[10] D. DeMille, Quantum Computation with Trapped Polar Molecules. Phys. Rev. Lett.. **88**. 067901. (2002)

[11] X.-F. Shi, Rydberg quantum computation with nuclear spins in two-electron neutral atoms, Frontiers of Physics, vol. **16**, no. 5, Apr. 2021.

[12] R.Blatt, C. Roos, Quantum simulations with trapped ions. Nature Phys **8**, 277–284 (2012).

[13] I.M. Georgescu, S. Ashhab, and Franco Nori Rev. Mod. Phys. 86, 153 (2014)

[14] Ma, H., Govoni, M. , Galli, G. Quantum simulations of materials on near-term quantum computers. npj Comput Mater **6**, 85 (2020).

[15] Faroukh, Yousuf. Quantum Computers Vs Conventional Computers: A Study on the Larger Scale. (2018)

[16] M. A. Nielsen and I. L. Chuang, quantum Computation and Quantum Info.: 10th Anni. Ed, Cambridge University Press40 W. 20 St. New York, NYUnited States, **708** (2011).

[17] Z. Wang, X. Gu, L.-A. Wu, and Y.-x. Liu, Quantum simulation of pairing hamiltonians with nearest-neighbor interacting qubits, Phys. Rev. A **93**, 062301 (2016).

[18] R. Babbush, D.W. Berry,J.R. McClean, et al. Quantum simulation of chemistry with sublinear scaling in basis size. npj Quantum Inf **5**, 92 (2019).

[19] C. Outeiral, M. Strahm, J. Shi, Garr M. Morris, Simon C. Benjamin, C. M. Deane, WIREs Comp. Mol. Science, (2020)

[20] J. Bardeen, L. N. Cooper, and J. R. Schrieffer Phys. Rev. **108**, 1175

[21] Y. Alhassid, K.N. Nesterov Mesoscopic superconductivity in ultrasmall metallic grains AIP Conf. Proc. 1619, **24** (2014)

[22] X.-D. Yang, A. M. Wang, F. Xu, and J. Du, Experimental simulation of a pairing Hamiltonian on an NMR quantum computer, Chem. Phys. Lett. **422**, 20-24 (2006).

[23] A.Di Paolo, T.E.Baker, A. Foley, et al. Efficient modeling of superconducting quantum circuits with tensor networks. npj Quantum Inf **7**, 11 (2021).

[24] Z.I.Alferov, The history and future of semiconductor heterostructures. Semiconductors **32**, 1–14 (1998).

[25] G. Ortiz, J. E. Gubernatis, E. Knille, and R. Laflamme, Quantum algorithms for fermionic simulations, Phys. Rev. A **64**, 022319 (2001).

[26] S. Lloyd, Universal quantum simulators, Science **273**, 1073-1078 (1996).

[27] A. Pathak, Elements of Quantum Computation and Quantum Communication, (2013).

[28] Wikipedia, Quantum logic gate, https://en.wikipedia.org/wiki/Quantum_logic_gate Accessed on February 2019.

[29] I. M. Georgescu, S. Ashhab, and F. Nori. Quantum Simulation, Rev. Mod. Phys. **86**, 153-185 (2014).

[30] Pedersen, Line Hjortshoj and Moller, Niels Martin and Molmer, Klaus. Fidelity of quantum operations.DOI=10.1016/j.physleta.2007.02.069

[31] M.H. Devoret, R.J. Schoelkopf. Superconducting circuits for quantum information: an outlook. Science. (2013)

[32] J. Clarke,F.K. Wilhelm. Superconducting quantum bits. Nature. (2008)

[33] J. Q. You and F. Nori, Phys. Today 58(11), **42** (2005)

[34] L.-A. Wu, M. S. Byrd and D. A. Lidar, Phys. Rev. Lett. **89**, 057904 (2002)

[35] T. P. Orlando, J. E. Mooij, L. Tian, C. H. van der Wal, L. S. Levitov, S. Lloyd, and J.J. Mazo, Phys. Rev. B **60**, 15398 (1999).

[36] J. Q. You, J. S. Tsai, and F. Nori, Phys. Rev. Lett. **89**, 197902 (2002).

[37] T. Ghosh, S. Sarkar, B. K. Behera, P. K. Panigrahi,An Open Idea to Secure Quantum Money Scheme From Quantum Sniffing Attack, DOI: 10.13140/RG.2.2.22807.73124 (2019)

[38] S. Barik, D. K. Kalita, B. K. Behera, and P. K. Panigrahi, Demonstrating Quantum Zeno Effect on IBM Quantum Experience, arXiv:2008.01070 (2020).

[39] S. Gangopadhyay, Manabputra, B. K. Behera, P. K. Panigrahi, Generalization and demonstration of an entanglement-based Deutsch-Jozsa-like algorithm using a 5-qubit quantum computer, Quantum Inf. Process. **17**, 160 (2018).

[40] K. Supriya, A. Banik, B. K. Behera, and P. K. Panigrahi, Experimental Demonstration of Delta, Scattering and Interaction Potentials in IBM Quantum Experience, DOI: 10.13140/RG.2.2.34192.15362 (2020)

[41] A. Singh, B. K. Behera, and P. K. Panigrahi, Designing a Quantum Router Based on System Hamiltonian: An IBM Quantum Experience, DOI: 10.13140/RG.2.2.21632.17923 (2020)

[42] M. Bindhani, B. K. Behera, and P. K. Panigrahi, Quantum Simulation of Jaynes-Cummings Model on IBM Q System, DOI: 10.13140/RG.2.2.14770.56006 (2020)

[43] S. Bhosale, B. K. Behera, and P. K. Panigrahi, Exploring Nature's ghost:Neutrino oscillations on IBM Q computer, DOI: 10.13140/RG.2.2.16560.71686 (2019)

[44] K. Sarkar, B. K. Behera, and P. K. Panigrahi, A robust tripartite quantum key distribution using mutually share Bell states and classical has values using a complete graph network architecture, DOI: 10.13140/RG.2.2.27559.39844 (2019)

[45] R. Agarwal, C. K. Sethi, N. K. Gupta, and P. K. Panigrahi, Comparison of advantages in quantum teleportation using cluster state and coined quantum walks, DOI: 10.13140/RG.2.2.35192.80648 (2020)

[46] A. Warke, B. K. Behera, and P. K. Panigrahi, Experimental Realization of Three Quantum Key Distribution Protocols, DOI: 10.13140/RG.2.2.15812.78725 (2019)

[47] R. Saini, A. Papneja, B. K. Behera, and P. K. Panigrahi, Experimental Realization of Differential Phase Shift Quantum Key Distribution on IBM QX, DOI: 10.13140/RG.2.2.10904.14089 (2019)

[48] B. K. Behera, A. Banerjee, P. K. Panigrahi, Experimental realization of quantum cheque using a five-qubit quantum computer, Quantum Inf. Process. **16**, 12 (2017).

[49] B. K. Behera, T. Reza, A. Gupta, and P. K. Panigrahi, Designing Quantum Router in IBM Quantum Computer, Quantum Inf. Process. **18**, 328 (2019).

[50] B. K. Behera, S. Seth, A. Das, and P. K. Panigrahi, Demonstration of Entanglement Purification and Swapping Protocol to Design Quantum Repeater in IBM Quantum Computer, Quantum Inf. Process. **18**, 108 (2019).

[51] R. McDermott, R. W. Simmonds, Matthias Steffen, K. B. Cooper, K. Cicak, K. D. Osborn, Seongshik Oh, D. P. Pappas, John M. Martinis, Science **307**, 1299 (2005).

[52] D. Loss and D.P. DiVincenzo Phys. Rev. A **57**, 120

[53] D.W. Leung, Isaac L. Chuang, F. Yamaguchi, and Y. Yamamoto Phys. Rev. A **61**, 042310.

[54] A.Houck, H. Türeci and J. Koch, On-chip quantum simulation with superconducting circuits. Nature Phys **8**, 292–299 (2012).

[55] D. J. Griffith, Quantum Mechanics.

[56] R. Barends, J. Kelly, A. Megrant , A. Veitia, D. Sank, E. Jeffrey, T.C. White, J. Mutus, A.G. Fowler , B. Campbell, Y.Chen , Z. Chen, B. Chiaro , A. Dunsworth, C. Neill, P.O'Malley , P.Roushan, A. Vainsencher, J. Wenner , A.N. Korotkov , A.N. Cleland, J.M. Martinis, Superconducting quantum circuits at the surface code threshold for fault tolerance. Nature. ;**508** (7497):500-3. (2014)

[57] F. Tacchino, A. Chiesa, S. Carretta, and D. Gerace, Quantum computers as universal quantum simulators: state of art and perspectives, Advanced Quantum Technologies **3**, 1900052 (2020)

[58] J. T. Barreirro, M. Mueller, P. Schindler, M. Hennrich, C. F. Roos, P. Zoller, and R. Blatt, An open system quantum simulator with trapped ions, Nature **470**, 486–491.

[59] J. B. Altepeter, D. F. V. James, and P. G. Kwiat, Quantum State Tomography.